COMPARISON OF LAM–ROTT AND BROWN–STEWARTSON EIGENSOLUTIONS OF THE BOUNDARY-LAYER EQUATIONS

by P. W. HAMMERTON

(*School of Mathematics, University of East Anglia, Norwich* NR4 7TJ)

Summary

In studies of the boundary layer on a flat plate, two very different sets of asymptotic eigenfunctions of the linearized unsteady boundary-layer equation have been analysed. One set, usually known as Lam–Rott eigenfunctions, decay exponentially with a shortening wavelength, while the other set, known as Brown–Stewartson modes, decay more slowly. Lam–Rott eigenfunctions have been extensively studied, and the presence of these eigenfunctions in the boundary-layer solution is important when studying the receptivity of the boundary layer to free-stream disturbances. In contrast, the Brown–Stewartson modes have been largely ignored. In this paper the two sets of eigensolutions are compared, and the presence of both Lam–Rott and Brown–Stewartson modes in numerical solutions of the boundary-layer equation is demonstrated.

1. Introduction

The boundary-layer flow on a flat plate subject to small time-periodic perturbations in the magnitude of the mainstream velocity was first addressed by Lighthill (**1**). Linearizing about the mean flow, a series solution valid close to the leading edge is obtained, together with an asymptotic solution valid far downstream. Far from the leading edge, a two-layer Stokes flow arises, determined entirely by the local conditions. However, the solution can also be supplemented by the addition of eigensolutions satisfying homogeneous boundary conditions, the magnitude of which are determined by conditions at an $O(1)$ distance from the leading edge.

Lam and Rott (**2**) obtained one set of eigensolutions using separation of variables, essentially anticipating the use of matched asymptotic expansions. Ackerberg and Phillips (**3**) later gave a systematic asymptotic analysis leading to the same set of eigensolutions. More recently Lam and Rott (**4**) presented a more general derivation of these eigenfunctions, taking account of mean pressure gradients. The essential character of these eigenfunctions is that they are exponentially damped with distance downstream, with shortening wavelength, and that the asymptotic structure is determined by behaviour close to the wall. The importance of these eigenfunctions was revealed by Goldstein (**5**) when considering the receptivity of a boundary layer, that is, how unsteady perturbations to the free stream flow speed seed disturbances in the boundary layer, which eventually lead to the transition of the boundary layer from laminar to turbulent flow. Disturbances in the free stream typically have a length scale much larger than that of Tollmien–Schlichting waves. Thus, the shortening wavelength of the Lam–Rott modes provides the key to understanding leading-edge receptivity. Moreover, Goldstein demonstrated that far downstream, the fastest decaying Lam–Rott mode matches on to the Orr–Sommerfeld mode which eventually grows. Study of receptivity of more realistic bodies, taking account of body thickness, has led to the development of generalized Lam–Rott eigenfunctions (**4**, **6**).

Analysis of the numerical solution of the unsteady boundary layer on a flat plate has led to the suggestion that the complete boundary-layer solution is the sum of the Stokes solution and a sequence of Lam–Rott eigenfunctions (**7**). However, for physical applications, the set of Lam–Rott modes does have unappealing features, notably the modes are inversely ordered far downstream. For this reason, Brown and Stewartson (**8**) developed an alternative set of eigensolutions which are correctly ordered. These modes propagate at the free-stream velocity, and the disturbances are concentrated at the outer edge of the boundary layer. However, the development of Brown–Stewartson modes far downstream does not appear to lead to the appearance of unstable disturbances. For this reason, the possible presence of Brown–Stewartson modes in the unsteady boundary layer has been overlooked in receptivity analyses.

The purpose of the present study is to compare the structures of the two sets of modes, and discuss methods by which the presence of such modes can be identified in numerical solutions of the linearized boundary-layer equation. We show that eigensolutions with the character of Brown–Stewartson modes can indeed be identified in numerical solutions, along with Lam–Rott modes.

2. Mathematical formulation

A semi-infinite flat plate is located at $\overline{y} = 0$, $\overline{x} > 0$, with a mainstream velocity parallel to the plate, $\mathbf{u} = (\overline{U}, 0)$, where

$$\overline{U} = U_0 \left(1 + \epsilon e^{-i\omega \overline{t}}\right), \qquad \epsilon \ll 1, \tag{1}$$

and bars denote dimensional variables. Non-dimensionalizing, the boundary-layer equation becomes

$$\psi_{yt} + \psi_y \psi_{yx} - \psi_x \psi_{yy} = U_t + \psi_{yyy}, \tag{2}$$

where

$$t = \omega \overline{t}, \qquad x = \frac{\omega \overline{x}}{U_0}, \qquad y = \left(\frac{\omega}{\nu}\right)^{\frac{1}{2}} \overline{y}, \qquad \psi = \left(\frac{\omega}{\nu U_0^2}\right)^{\frac{1}{2}} \overline{\psi}, \qquad U = \frac{\overline{U}}{U_0}. \tag{3}$$

Here ν is the kinematic viscosity and $\overline{\psi}$ is the dimensional stream function. The boundary-layer equation (2) is to be solved in the small-ϵ limit, subject to the boundary conditions

$$\begin{aligned}
\psi(x, 0) &= \psi_y(x, 0) = 0, \\
\psi_y(x, y) &\to 1 + \epsilon e^{-it} \quad \text{as} \quad y \to \infty, \\
\psi_y(0, y) &= 1 + \epsilon e^{-it}, \quad y > 0.
\end{aligned} \tag{4}$$

Defining new boundary-layer variables, $\xi = x$ and $\eta = y/(2x)^{1/2}$, and taking the limit $\epsilon \to 0$, we obtain

$$\psi = (2\xi)^{1/2} \left(F(\eta) + \epsilon G(\xi, \eta) e^{-it} + O(\epsilon^2)\right), \tag{5}$$

where $F(\eta)$ is the Blasius function and $G(\xi, \eta)$ satisfies the linearized unsteady boundary-layer equation

$$G_{\eta\eta\eta} + F G_{\eta\eta} + F_{\eta\eta} G - 2\xi (F_\eta G_{\eta\xi} - F_{\eta\eta} G_\xi - i G_\eta) = 2\xi i, \tag{6}$$

with boundary conditions

$$G(\xi, 0) = G_\eta(\xi, 0) = 0, \qquad G_\eta(\xi, \eta) \to 1 \quad \text{as} \quad \eta \to \infty. \tag{7}$$

In this paper we consider the form of the solution of (6) far downstream from the leading edge. The particular solution, determined entirely by conditions far downstream, is the classical Stokes-layer solution (1). A two-layer structure develops, with inner deck $\eta = O(\xi^{-1/2})$. Moving downstream, the inner layer becomes thinner relative to the overall boundary-layer thickness, but in terms of the original variables it approaches a uniform thickness, $\bar{y} = O\big((\nu/\omega)^{1/2}\big)$. At the outer edge of the boundary layer, the Stokes solution takes the form

$$G_{\mathrm{St}} \sim \eta - \frac{1+i}{2}\frac{1}{\xi^{1/2}} + i\beta\frac{1}{2\xi} + \frac{13\lambda}{32}\frac{1}{\xi^2} - \frac{39i\lambda}{64}\frac{1}{\xi^3} + O(\xi^{-7/2}), \tag{8}$$

where $\lambda \equiv F''(0) \approx 0\cdot4696$ and $\beta = \lim_{\eta\to0}(\eta F' - F) \approx 1\cdot217$. The limit of $G(\xi, \eta)$ as $\eta \to \infty$ provides a convenient basis for the comparison of asymptotic and numerical results in section 3.

It is clear that the Stokes solution is independent of upstream boundary conditions, while the nature of the partial differential equation (6) is such that the conditions close to the leading edge must influence the solution far downstream. Thus the full solution takes the form

$$G = G_{\mathrm{St}} + \sum_i C_i G_i(\xi, \eta), \tag{9}$$

where $G_i(\xi, \eta)$ are locally determined eigenfunctions satisfying homogeneous boundary conditions, and the constants C_i are determined by conditions close to the leading edge.

Two contrasting sets of eigenfunctions have been formulated (2, 8). The purpose of the present paper is the comparison of these two sets of eigenfunctions, and in particular the identification of them in the numerical solutions of the boundary-layer equation (6). Here we summarize the asymptotic structure of the two sets of eigenfunctions.

2.1 Lam–Rott eigenfunctions

Lam–Rott eigenfunctions (2) are obtained using separation of variables. As for the Stokes solution, a two-layer structure arises with the inner layer scaling on $\xi^{-1/2}$. The form of the solution in both layers is given elsewhere (3, 5); here we restrict attention to the streamwise variation at the outer edge of the boundary layer, when the nth eigenfunction takes the form

$$G_n^{\mathrm{LR}}(\xi, \eta) \sim \xi^{\tau_n} \exp\left(-\gamma_n \xi^{3/2}\right) \tag{10}$$

as $\eta \to \infty$, where

$$\tau_n = -\frac{889 - 16\rho_n^3}{1260}, \qquad \gamma_n = \left(\frac{2}{\rho_n}\right)^{3/2}\frac{e^{-i\pi/4}}{3\lambda} \tag{11}$$

and ρ_n is the nth positive root of $\mathrm{Ai}'(-\rho) = 0$. The presence of the algebraic variation term ξ^{τ_n} was first identified by Goldstein (5), and is determined by a solvability condition at higher order in the large-ξ asymptotic expansion. The simplified form of the expression for τ_n follows from Hammerton and Kerschen (6).

From (10), the wavelength of the nth Lam–Rott mode is given by

$$\lambda_n(\xi) = \frac{3\lambda\rho_n^{3/2}}{2}\frac{1}{\xi^{1/2}}, \tag{12}$$

Table 1 Numerical values of parameters appearing in first five Lam–Rott eigenfunctions

ρ_n	τ_n	α_n	ξ_n^M	$A_n(\xi_n^M)$
1·0188	-0·6921	-1·3805		
3·2482	-0·2704	-0·2425		
4·8201	0·7165	-0·1342	2·3318	1·1376
6·1633	2·2674	-0·0928	6·4267	14·9816
7·3722	4·3823	-0·0709	11·9275	2811·7761
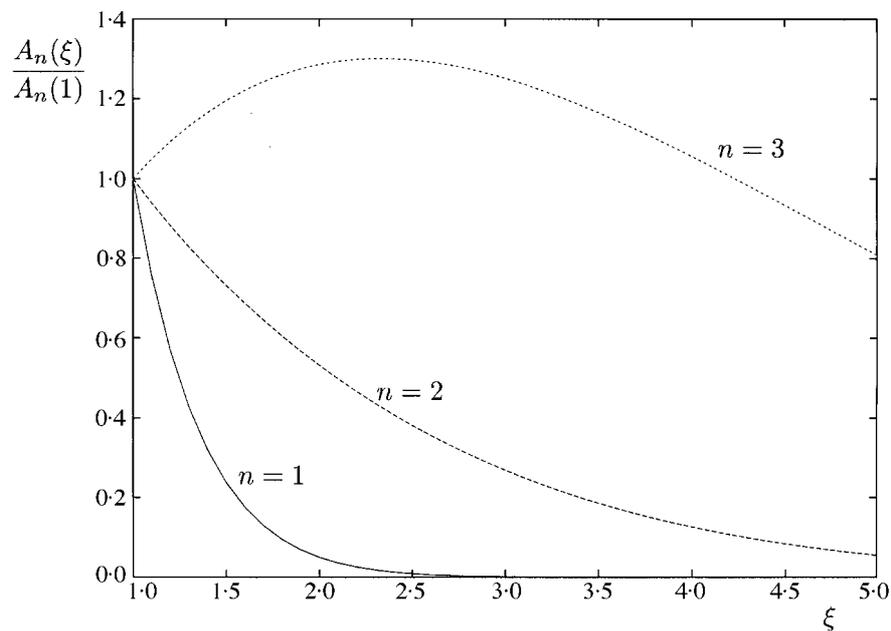
Fig. 1 The amplitude of the first three Lam–Rott eigensolutions as a function of distance downstream from the leading edge

and the amplitude is given by

$$A_n(\xi) = \xi^{\tau_n} \exp\left(-\alpha_n \xi^{3/2}\right), \qquad \alpha_n = \frac{2}{3\lambda\rho_n^{3/2}}. \tag{13}$$

Hence all the Lam–Rott modes are exponentially damped at large distances downstream, with wavelength decreasing with distance downstream. Numerical values of ρ_n for n from 1 to 5, are given in Table 1, and the streamwise amplitude variation (normalized at $\xi = 1$) is illustrated in Fig. 1 for the first three Lam–Rott eigenfunctions.

Lam–Rott modes have been used in the study of leading-edge receptivity, as described in section

1, since a mechanism of wavelength conversion is needed and from (12) the Lam–Rott modes provide the required shortening of the wavelength with distance downstream. However, other features of the Lam–Rott modes prove less physically appealing. Since α_n is a decreasing function of n, for large ξ the Lam–Rott modes are inversely ordered, so

$$|G_{n+1}^{\mathrm{LR}}| > |G_n^{\mathrm{LR}}|. \tag{14}$$

This was noted by Brown and Stewartson (**8**) in connection with the original formulations of the Lam–Rott modes (**2**, **3**). When the algebraic amplitude variation calculated by Goldstein (**5**) is included, the situation is even worse, since from Table 1 it is seen that for $n \geq 3$, $\tau_n > 0$, and hence these Lam–Rott modes grow algebraically before decaying. The maximum amplitude occurs when $\xi = \xi_n^M$, where

$$\xi_n^M = (\lambda \tau_n)^{2/3} \rho_n. \tag{15}$$

From Table 1, the maximum amplitude as a function of downstream distance increases very rapidly with n. This casts doubt on the validity of expressing the solution as an infinite sum of such modes. However, closer examination of the asymptotic structure of the Lam–Rott modes shows that the width of the inner layer of the nth mode scales on $(\rho_n/\xi)^{1/2}$ rather than $\xi^{-1/2}$. Hence the width of the inner layer is larger for the higher modes, and since the inner layer is assumed thin compared to the whole boundary layer, the asymptotic form of the higher eigensolutions only becomes valid further downstream.

2.2 *Brown–Stewartson eigenfunctions*

The alternative set of eigensolutions obtained by Brown and Stewartson (**8**) is based on the assumption that disturbances in the boundary layer propagate with a phase speed close to the free-stream velocity, and that the form of the eigensolution is dominated by the behaviour close to the outer edge of the boundary layer, rather than by the layer close to the wall, as in the case of the Lam–Rott modes. Analysis of eigensolutions of this form is motivated by the results of Stewartson (**9**, **10**) for an impulsively started, semi-infinite flat plate. In this case, disturbances due to the leading edge travel downstream with the free-stream velocity and spread inwards from the outer edge of the boundary layer. The requirement that the disturbance is convected by the free stream means that the dominant variation of $G(\xi, \eta)$ with ξ is proportional to $e^{i\xi}$. Hence, we write

$$G^{\mathrm{BS}}(\xi, \eta) = e^{i\xi} g(\xi, \eta), \tag{16}$$

where $g(\xi, \eta)$ satisfies the homogeneous equation

$$g_{\eta\eta\eta} + F g_{\eta\eta} + F_{\eta\eta} g - 2\xi \left(i(F_\eta - 1)g_\eta + F_\eta g_\xi - F_{\eta\eta} g_\xi - i F_{\eta\eta} g_\eta \right) = 0, \tag{17}$$

with boundary conditions $g = g_\eta = 0$ at $\eta = 0$ and $g_\eta \to 0$ exponentially as $\eta \to \infty$. Since we are considering solutions dominated by the behaviour close to the outer edge of the boundary layer, we consider the region where $\xi(1 - F_\eta) = O(1)$. Examining the large-η form of the Blasius function,

$$F_\eta(\eta) \sim 1 - \frac{\alpha}{\eta - \beta} e^{-(\eta - \beta)^2/2}, \quad \alpha \approx 0{\cdot}331, \quad \beta \approx 1{\cdot}217, \tag{18}$$

the region $\xi(1 - F_\eta) = O(1)$ corresponds to $\eta - \beta = O(\eta_0)$, where $\eta_0 = (\log(\alpha\xi))^{1/2}$. The
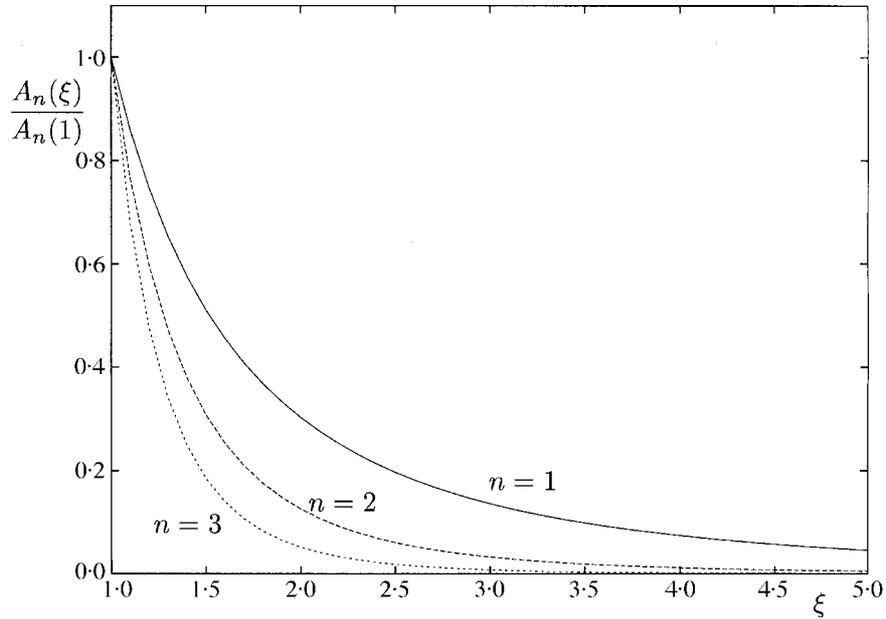
Fig. 2 The amplitude of the first three Brown–Stewartson eigenfunctions, normalized at $\xi = 1$, as a function of distance downstream from the leading edge

asymptotic form of the solution in this region is given in (**8**). Here we do not give the mode shape, but the disturbance is restricted to a layer of width $O(1/\eta_0)$, centred on $\eta = \beta + \eta_0$. Outside this layer, the horizontal perturbation velocity g_η is exponentially small. Similarly, in the lower part of the boundary layer the disturbance is exponentially small. The large-η limit of the nth Brown–Stewartson mode takes the form

$$G_n^{\mathrm{BS}}(\xi, \eta) \sim A e^{i\xi - \mu_n(\xi)}, \tag{19}$$

where

$$\mu_n(\xi) = \tfrac{1}{8}l^2 + \frac{3}{2^{10/3}}\kappa_n l^{4/3} - \tfrac{3}{8}(\log l)l + \tfrac{1}{2}(\gamma - \tfrac{1}{4}\log 2 + \tfrac{9}{4})l$$
$$+ \frac{2^{1/3}}{10}\kappa_n^2 l^{2/3} + o(l^{1/3+\delta}) \tag{20}$$

as $\xi \to \infty$. Here $l = \log(-\alpha i \xi)$, γ is Euler's constant and κ_n is the nth positive root of $\mathrm{Ai}(-\kappa) = 0$. Hence all modes are damped, but the decay rate is less than exponential. The amplitude of the first three Brown–Stewartson eigenfunctions at the outer edge of the boundary layer is plotted against streamwise distance in Fig. 2. Comparing Figs 1 and 2, we see that although the Lam–Rott modes are exponentially smaller than the Brown–Stewartson modes for large ξ, over the moderate ranges considered here ($1 < \xi < 5$), the amplitude variation of the first two modes of the two sets of eigenfunctions is similar.
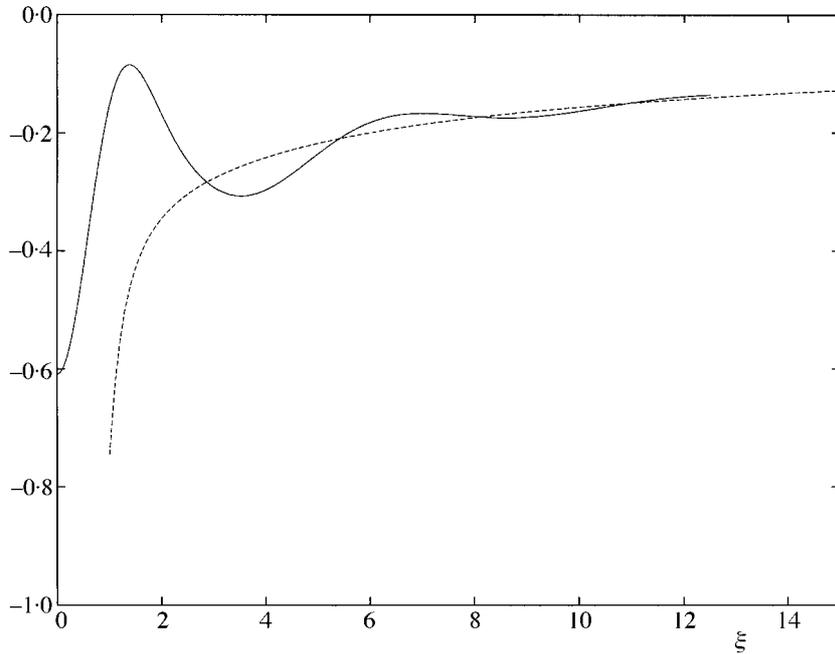
Fig. 3 The real part of $\delta(\xi)$ from the numerical solution (——————) and the asymptotic result (- - - - - - - - -) for the Stokes solution (8)

3. Comparison with numerical results

Having described the large-ξ asymptotic form of the unsteady boundary-layer solution, we now consider whether the presence of either Lam–Rott or Brown–Stewartson eigenfunctions can be identified from numerical solutions of the boundary-layer equation.

The linearized unsteady boundary-layer equation (6) was solved using the Keller box scheme (**11**), marching downstream from the solution at the leading edge (**1**),

$$G(0, \eta) = \tfrac{1}{2}(\eta F' + F). \tag{21}$$

The value of the solution at the outer edge of the boundary layer provides a convenient comparison between numerical and asymptotic results, hence we define

$$\delta(\xi) = \lim_{\eta \to \infty} (G(\xi, \eta) - \eta). \tag{22}$$

Confirmation of the large-ξ form of the Stokes solution is straightforward. In Fig. 3, the real part of $\delta(\xi)$ obtained from the numerical solution is plotted together with the asymptotic result from (8). Thus it is clear that (8) is indeed the large-ξ expansion for $\lim_{\eta \to \infty} G(\xi, \eta)$.

Identification of eigensolutions from numerical results is more difficult. Formally, the asymptotic form of the Lam–Rott eigenfunctions at the outer edge of the boundary layer (10) is only valid in the limit $\xi \to \infty$, in which case the Lam–Rott modes are exponentially smaller than the Stokes solution. Hence such modes cannot be recognised in large-ξ numerical solutions. Although the Brown–Stewartson modes decay more slowly than Lam–Rott modes, they are still smaller than the Stokes

solution by a factor $|\xi^{-1/2}e^{-\mu_n(\xi)}|$. However, progress can be made by comparing numerical and asymptotic solutions for moderate values of ξ. Ackerberg and Phillips (**3**) considered the difference between the numerical solution $G_{\text{num}}(\xi, \eta)$ and the asymptotic Stokes solution $G_{\text{St}}(\xi, \eta)$ at the outer edge of the boundary layer. By considering results in the range $3 < \xi < 10$, and assuming that the full solution consists of the Stokes solution and a sum of a number of Lam–Rott eigensolutions

$$\delta_{\text{num}} - \delta_{\text{St}} = \sum_n C_n \delta_n^{\text{LR}}, \tag{23}$$

the complex coefficients C_n were determined by a best-fit estimate. From a theoretical viewpoint, such an approach seems unlikely to succeed since the Lam–Rott eigenfunctions are inversely ordered. Ackerberg and Phillips (**3**) assumed that only three eigenfunctions were present, but no consistent results for C_n could be obtained, unsurprisingly since the algebraic variation was omitted from the Lam–Rott modes.

In the light of the failure to match numerical results to asymptotic Lam–Rott eigenfunctions, Brown and Stewartson (**8**) attempted to compare the numerical results of Ackerberg and Phillips with the streamwise variation of the first Brown–Stewartson mode. They showed that the numerical results were in approximate agreement with the first Brown–Stewartson mode. However, as noted in section 2, the streamwise amplitude variation of the first two Brown–Stewartson modes is very similar to that of the first two Lam–Rott modes. Hence the comparisons made do not provide convincing evidence of the presence of a Brown–Stewartson mode. Moreover, any attempt to estimate the coefficients in an expansion of the form

$$\delta_{\text{num}} - \delta_{\text{St}} = \sum_n D_n \delta_n^{\text{BS}} \tag{24}$$

is impossible unless the $O(1)$ variation of $\delta_n^{\text{BS}}(\xi)$ can be determined.

Goldstein *et al.* (**7**) repeated the analysis of Ackerberg and Phillips using the corrected expression for the Lam–Rott eigenmodes including algebraic amplitude variation. Considering the difference between numerical and asymptotic results in Fig. 3, and the streamwise variation of the Lam–Rott modes, it is clear that the coefficients C_n of the higher modes must be small. Consistent estimates for C_n were obtained by curve fitting for $1 < \xi < 6$, based on five or six eigenfunctions being present (**7**). These results are sufficiently convincing to suggest that Brown–Stewartson modes may be absent from the numerical solutions. However, as noted above, over the moderate values of ξ considered, it is difficult to distinguish between the first two modes of each set of eigensolutions. Hence, the numerical analysis of earlier authors (**3, 7, 8**) does not conclusively prove the existence or otherwise of either set of eigenfunctions.

Greater insight can be gained by considering the analytic continuation of the eigensolutions into the complex ξ-plane. If $\arg(\xi) = \theta$, the leading-order amplitude variation of the eigensolutions is given by

$$\log\left(|\delta_n^{\text{LR}}|\right) = -\frac{1}{3\lambda}\left(\frac{2}{\rho_n}\right)^{3/2}\cos\left(\tfrac{3}{2}\theta - \tfrac{1}{4}\pi\right)|\xi|^{3/2} + O(\log(|\xi|)), \tag{25}$$

$$\log\left(|\delta_n^{\text{BS}}|\right) = \cos\left(\tfrac{1}{2}\pi + \theta\right)|\xi| + O(\log(|\xi|)^2). \tag{26}$$

Hence, if $-\tfrac{5}{6}\pi < \theta < -\tfrac{1}{6}\pi$, then all the Lam–Rott eigenfunctions grow exponentially with increasing $|\xi|$ and $|G_{n+1}^{\text{LR}}| < |G_n^{\text{LR}}|$. Similarly, if $-\pi < \theta < 0$, then the Brown–Stewartson modes

grow exponentially. Consideration of the higher-order terms for the growth rate of the Brown–Stewartson modes (20) shows that the ordering of the eigenfunctions is unaltered by extending into the complex ξ-plane. If we *assume* that the sets of Lam–Rott and Brown–Stewartson modes are independent, and that together they form a complete set of eigensolutions, then

$$\delta_{\text{num}} - \delta_{\text{St}} = \sum_n C_n \delta_n^{\text{LR}} + \sum_n D_n \delta_n^{\text{BS}}. \tag{27}$$

It then follows that for $-\frac{1}{6}\pi < \theta < 0$, the Brown–Stewartson modes are large, all the Lam–Rott modes are exponentially small, and

$$\delta_{\text{num}} \sim D_1 \delta_1^{\text{BS}} \tag{28}$$

as $|\xi| \to \infty$. Similarly, if $-\frac{5}{6}\pi < \theta < -\frac{1}{6}\pi$, then both the Brown–Stewartson modes and the Lam–Rott modes are large, but the Lam–Rott modes are dominant and

$$\delta_{\text{num}} \sim C_1 \delta_1^{\text{LR}}. \tag{29}$$

Thus, extending the analysis into the complex ξ-plane provides a convenient method for detecting the presence of the first Lam–Rott mode and the first Brown–Stewartson mode. Using the Keller box scheme mentioned earlier, numerical results were obtained for $\arg(\xi) = -\frac{1}{5}\pi$ and $\arg(\xi) = -\frac{1}{10}\pi$. In the first case, when the first Lam–Rott mode should be dominant, the exponential growth proportional to $|\xi|^{3/2}$ predicted by (25) and (29) was seen in the numerical solution. These results are not reproduced here, since the rapid growth with ξ limits the numerical accuracy for large ξ. To increase the accuracy over a larger streamwise range, the leading-order growth was extracted by solving the linearized unsteady boundary-layer equation for $\hat{G} = Ge^{-\gamma_1\xi^{3/2}}$ rather than for G. Defining

$$f(\xi) = \text{Re}\left(\log(\hat{\delta}_{\text{num}}\xi^{-\tau_1})\right), \tag{30}$$

in Fig. 4 we plot $f(\xi)$ as a function of $|\xi|$. Since $f(\xi)$ tends to a constant as $|\xi|$ becomes large, we see that the numerical solution agrees with the asymptotic form (29) with $|C_1| \approx e^{-0.1} \approx 1.1$. The oscillation in $f(\xi)$ for $\xi < 4$ shows that for this particular value of $\arg(\xi)$, the Lam–Rott mode only becomes large compared to the Stokes solution when $\xi > 4$. The accuracy of the numerical evaluation of C_1 can be improved using a large-ξ extrapolation as described in (6). Taking account of higher-order terms in the asymptotic analysis,

$$f(\xi) \sim \log|C_1| + \frac{k}{|\xi|}, \tag{31}$$

where k is known. This then allows a more accurate estimation, $|C_1| \approx 0.950$, in good agreement with (7), hence validating the present numerical scheme. When $\arg(\xi) = -\frac{1}{10}\pi$, we expect the first Brown–Stewartson mode to be dominant. Direct numerical solution reveals the expected exponential growth rate proportional to $|\xi|$. As before, numerical accuracy is improved by extracting this leading-order growth and so solving for $\widetilde{G} = e^{-i\xi}G$. In Fig. 5 we plot $f^{(j)}(\xi)$ for $j = 0, 1, \ldots, 5$, where

$$f^{(j)}(\xi) = \text{Re}\left(\log(\widetilde{\delta}_{\text{num}}) + \mu_1^{(j)}(\xi)\right), \tag{32}$$

and $\mu_1^{(j)}(\xi)$ is the sum of the first j terms in the expansion for $\mu_1(\xi)$ given by (20). As noted
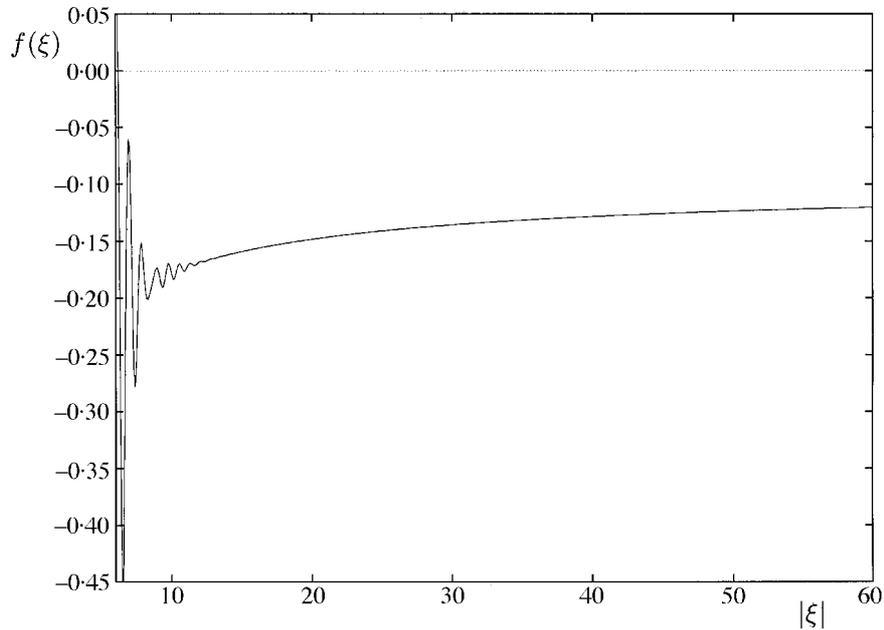
Fig. 4 Variation of $f(\xi)$, defined in (30), as a function of $|\xi|$ for $\arg(\xi) = -\frac{1}{5}\pi$

earlier, the $O(1)$ variation of the Brown–Stewartson mode has not been calculated. However, the inclusion of the additional terms in the amplitude variation given by (20) reduces the streamwise variation of the function. While this comparison does not completely validate all terms in the asymptotic expansion (20), it does demonstrate that the numerical solution has the character of the Brown–Stewartson mode. From Fig. 5, it is clear that $\widetilde{\delta}_{num}$ gets extremely small for large $|\xi|$, and so comparison of numerical and asymptotic results over larger streamwise ranges is improved by solving for $\hat{G} = e^{-i\xi + \mu_1^{(5)}} G$.

Conclusive evidence of the presence of Lam–Rott and Brown–Stewartson modes comes from considering the variation in the streamwise perturbation velocity, ψ_η, across the boundary layer at various stations downstream. Results for $\arg(\xi) = -\frac{1}{10}\pi$ and $-\frac{1}{5}\pi$ are plotted in Fig. 6. For easy comparison, the mode shapes are normalized so that the maximum amplitude is one in each case. In Fig. 6a, where $\arg(\xi) = -\frac{1}{5}\pi$ the disturbance is restricted to $0 < \eta < 4$, and the development of an inner layer close to the wall can be seen. The thickness of the inner layer decreases with increasing ξ, proportional to $\xi^{-\frac{1}{2}}$, in agreement with the structure of the Lam–Rott modes. Excellent agreement can be obtained between the numerical solution and a composite expansion formed from the two-layer asymptotic form. When $\arg(\xi) = -\frac{1}{10}\pi$ the mode shape is completely different. The solution is small over the inner part of the boundary layer and all velocity perturbation occurs in a relatively narrow layer, the position of which slowly moves away from the plate as the distance downstream is increased. Clearly this result is in agreement with the asymptotic form of the Brown–Stewartson modes. Attempts to make quantitative comparisons between the numerical results and the position
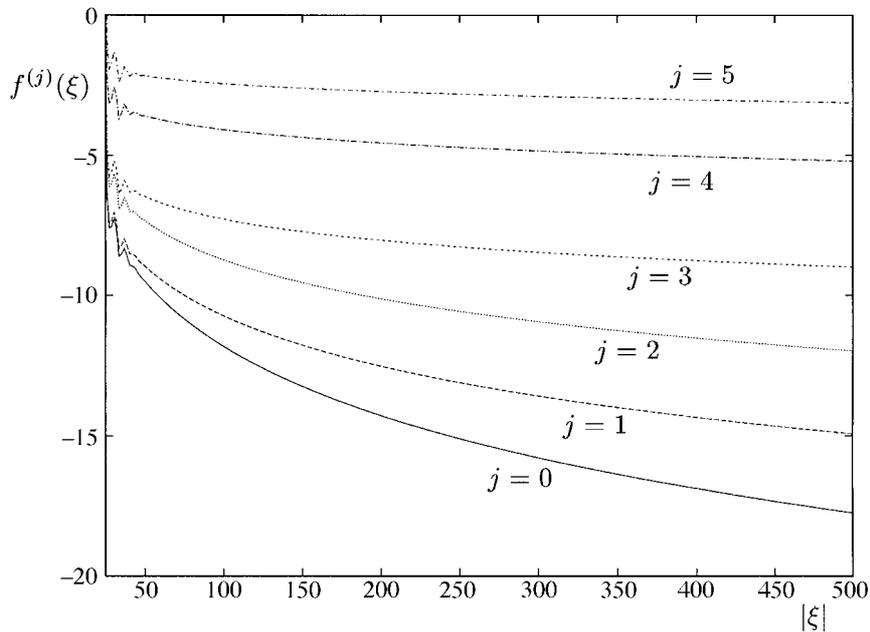
Fig. 5 The first six functions $f^{(j)}(\xi)$, defined in (32), as a function of $|\xi|$ for $\arg(\xi) = -\frac{1}{10}\pi$

of maximum velocity perturbation are hampered by the need to continue the numerical solution up to extremely large values of $|\xi|$ in order to obtain significant variation in $\eta_0 = (\log(\alpha\xi))^{1/2}$.

4. Conclusions

In this paper we have shown that both Brown–Stewartson and Lam–Rott eigensolutions have a role to play in analysing the solution of the linearized unsteady boundary-layer equation. It may be that the two sets of eigensolutions are not independent (**7**), though this lies beyond the scope of the present paper. Up to now, most attention has focused on Lam–Rott modes since the wavelength shortening explains the lengthscale conversion from free-stream disturbances to shorter Tollmien–Schlichting waves. Receptivity calculations (**7, 6**) have investigated how changes in the free-stream forcing close to the leading edge affect the coefficient C_1 of the Lam–Rott mode that matches onto the unstable Tollmien–Schlichting mode of the Orr–Sommerfeld equation. In these calculations Brown–Stewartson modes are ignored, though the presence of such modes should not invalidate the analysis of receptivity. Thus, in some sense, the Lam–Rott modes can be considered the more useful set of eigenfunctions. However, at this point in time the physical significance of Brown–Stewartson modes is unclear. Now that their presence has been identified in numerical solutions, further investigation seems worthwhile.

References

1. M. J. Lighthill, The response of laminar skin friction and heat transfer to fluctuations in the free-stream velocity. *Proc. R. Soc.* A **224** (1954) 1–23.
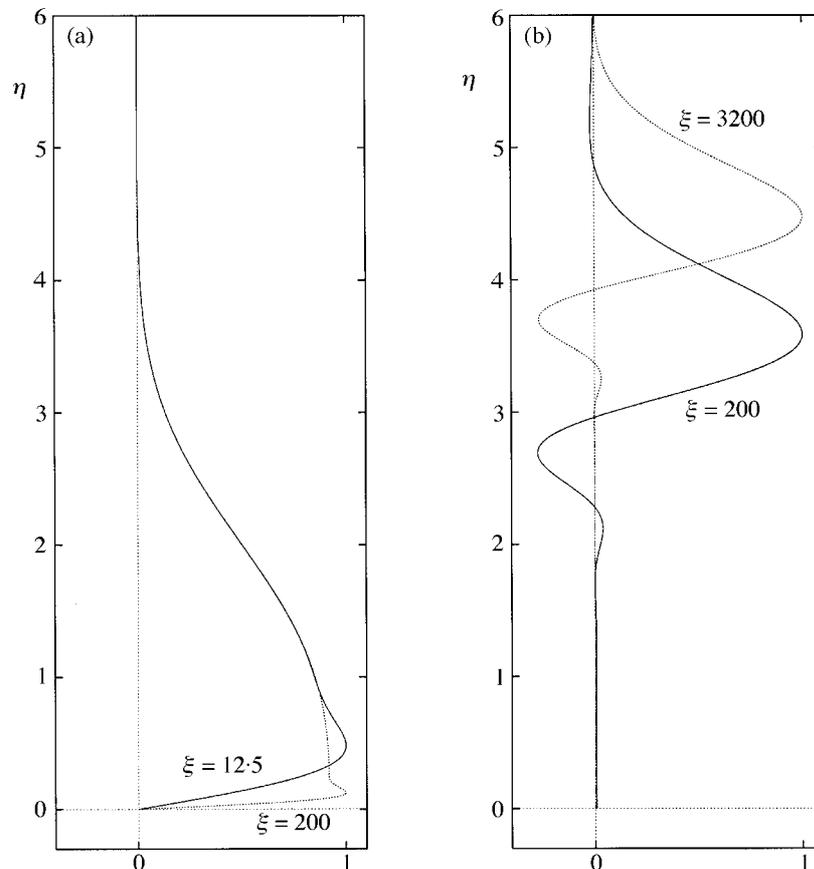
Fig. 6 The real part of $G_\eta(\xi, \eta)$ (normalized by its maximum amplitude) obtained from numerical solutions at various downstream positions when (a) $\arg(\xi) = -0{\cdot}2\pi$ and (b) $\arg(\xi) = -0{\cdot}1\pi$

2. S. H. Lam and N. Rott, Theory of linearized time-dependent boundary layers. *Cornell Univ. Grad. School of Aero. Engineering Rep.* AFOSR TN–60–1100 (1960).

3. R. C. Ackerberg and J. H. Phillips, The unsteady laminar boundary layer on a semi-infinite flat plate due to small fluctuations in the magnitude of the free-stream velocity. *J. Fluid Mech.* **51** (1972) 137–157.

4. S. H. Lam and N. Rott, Eigen-functions of linearized unsteady boundary layer equations. *J. Fluids Eng.* **115** (1993) 597–602.

5. M. E. Goldstein, The evolution of Tollmien–Schlichting waves near a leading edge. *J. Fluid Mech.* **127** (1983) 59–81.

6. P. W. Hammerton and E. J. Kerschen, Boundary-layer receptivity for a parabolic leading edge. *Ibid.* **310** (1996) 243–267.

7. M. E. Goldstein, P. M. Sockol and J. Sanz, The evolution of Tollmien–Schlichting waves near

a leading edge. Part 2. Numerical determination of amplitudes. *J. Fluid Mech.* **129** (1983) 443–453.

8. S. N. Brown and K. Stewartson, On the propagation of disturbances in a laminar boundary layer. *Proc. Camb. phil. Soc.* **73** (1973) 493–514.

9. K. Stewartson, On the impulsive motion of a flat plate in a viscous fluid I. *Q. Jl Mech. appl. Math.* **4** (1951) 182–198.

10. ——, On the impulsive motion of a flat plate in a viscous fluid II. *Ibid.* **26** (1973) 143–152.

11. H. B. Keller and T. Cebeci, Accurate numerical methods for boundary layer flows–I. Two-dimensional laminar flows. In *Proceedings of the Second International Conference on Numerical Methods in Fluid Mechanics* (ed. M. Holt; Springer, Berlin 1970) 92–100.